

Peridynamic Approach for Metal Quenching Problem to simulate thermo-mechanical effects

A thesis submitted in partial fulfillment of the requirements for
the award of the degree of

B.Tech

in

Mechanical Engineering

By

Manu Aatitya R P (111117058)

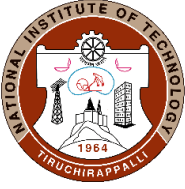
Yogeesh S (111117094)

Sriranga V (111117108)



**MECHANICAL ENGINEERING
NATIONAL INSTITUTE OF TECHNOLOGY
TIRUCHIRAPPALLI – 620015**

MAY 2021



National Institute of Technology Tiruchirappalli

Tanjore Road, Tiruchirappalli – 620 015, Tamil Nadu, INDIA.

Department of Mechanical Engineering

www.nitt.edu

Dr.-Ing. Ashok Kumar Nallathambi

Assistant Professor

Automobile Lab

Mobile: +91 95003 10739

Email : nashok@nitt.edu

January 19, 2021

B.Tech Final Year Project

This is to certify that the following THREE students showed interest and agreed to work under my guidance in the following topic:

Peridynamic approach for metal quenching problem to simulate thermomechanical effects

for their final year B. Tech degree project during the period of Jan/2021 – May/2021.

| S.No | Name | Roll No |
|------|------------------|-----------|
| 1 | Manu Aatitya R P | 111117058 |
| 2 | Yogeesh S | 111117094 |
| 3 | Sriranga V | 111117108 |

Sincerely

Ashok Kumar Nallathambi

Group No:

BONAFIDE CERTIFICATE

This is to certify that the project titled **Peridynamic Approach for Metal Quenching Problem to simulate thermo-mechanical effects** is a bonafide record of the work done by

Manu Aatitya R P

111117058

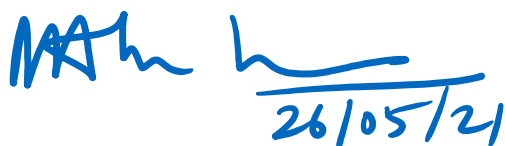
Yogeesh S

111117094

Sriranga V

111117108

in partial fulfillment of the requirements for the award of the degree of **Bachelor of Technology in Mechanical engineering** of the **NATIONAL INSTITUTE OF TECHNOLOGY, TIRUCHIRAPPALLI**, during the year 2017-2021.



Dr.-Ing. Ashok Kumar Nallathambi
Project Guide

Dr. AR. Veerappan
Head of the Department

Project Viva-voce held on _____

Internal Examiner

External Examiner

ABSTRACT

Peridynamics is a new modeling concept of non-local interactions for solid structures. The formulations of Peridynamic theory are based on integral equations rather than differential equations. Peridynamic theory might be defined as continuum version of molecular dynamics.

In this work, the peridynamic theory developed is applied to model thermo-mechanical effects, especially **conduction** and **mechanical loading**. MATLAB codes are generated to simulate thermo-mechanical problems in various domain configurations like completely solid structures and structures with discontinuities like cracks and holes. The simulation data is validated against solutions from other numerical methods (FEM, FDM and FVM) and analytical solutions (in special cases). A specific industrial problem of billet quenching in Direct Chill (DC) casting process has also been simulated using a simplified model using the peridynamic approach and compared against experimental Temperature profile data. The results show good agreement.

Keywords : Peridynamics, non-local continuum mechanics, Nonlocal elasticity, Material model, Crack dynamics - crack formation and growth, iterative approach,

ACKNOWLEDGEMENTS

We would like to express our deepest gratitude to the following people for guiding us through this course and without whom this project and the results achieved from it would not have reached completion.

We would like to show our deep gratitude to our project guide **Prof Dr.–Ing. Ashok Kumar Nallathambi** for providing us with an opportunity to work with him and for his constant guidance throughout the project. He greatly helped us understand the concepts involved and pushed us to think more critically. His valuable feedback helped us a lot in avoiding potential pitfalls and dealing with errors that did occur.

We would like to express our most sincere thanks to **Mr. Jijo Prasad** for his constant support and motivation, without which we wouldn't have been able to complete the project in time. His suggestions helped us analyse phenomena from different point of views and tackle problems.

We are also thankful to the faculty and staff members of the Department of Mechanical Engineering, our individual parents and our friends for their constant support and help.

TABLE OF CONTENTS

| Title | Page No. |
|--|----------|
| ABSTRACT | i |
| ACKNOWLEDGEMENTS | ii |
| TABLE OF CONTENTS | iii |
| LIST OF FIGURES | v |
| NOMENCLATURE | vii |
| CHAPTER 1 INTRODUCTION | 1 |
| 1.1 About Peridynamics | 1 |
| 1.2 Fundamental equation of bond-based Peridynamics | 1 |
| 1.2.1 Peridynamics formulation of Mechanics: | 1 |
| 1.2.2 Peridynamics formulation of Heat Transfer: | 3 |
| 1.3 Need for a new computational model | 4 |
| CHAPTER 2 Peridynamic Fomulation for simulating Thermal Effects | 5 |
| 2.1 1D Steady State Conduction | 5 |
| 2.1.1 Analytical Solution: | 5 |
| 2.1.2 Peridynamic Simulation: | 5 |
| 2.2 2D Steady State Conduction | 6 |
| 2.2.1 Analytical Solution: | 6 |
| 2.2.2 Peridynamic Solution: | 6 |
| 2.3 2D Transient Conduction profile with crack in domain | 7 |
| 2.3.1 Problem definition : | 7 |
| 2.3.2 Effect on increasing number of nodes: | 8 |
| 2.4 Crack propagation without mechanical coupling | 9 |

| | | |
|-------------------|--|-----------|
| 2.5 | Metal Quenching in Direct Chill Casting Process | 10 |
| 2.5.1 | Peridynamics Results: | 11 |
| 2.5.2 | Comparison | 13 |
| CHAPTER 3 | Peridynamic Formulation for simulating Mechanical Effects . . . | 15 |
| 3.1 | Mechanical damage formulation | 15 |
| 3.2 | 2D Plate subjected to Mechanical displacement | 16 |
| 3.3 | 2D Plate with hole subjected to Mechanical Displacement | 17 |
| 3.4 | 2D Plate with crack subjected to Mechanical Displacement | 18 |
| CHAPTER 4 | Conclusion and Scope for future Work | 20 |
| 4.1 | Conclusion | 20 |
| 4.2 | Future Work | 20 |
| APPENDIX A | Peridynamics - Matlab Implementation | 21 |
| A.1 | Peridynamics Simulation Overview | 21 |
| A.2 | Volume Correction for Interactions: | 21 |
| A.3 | Surface Correction for Interactions: | 22 |
| A.4 | Remove Interactions crossing Crack: | 23 |
| REFERENCES | | 25 |

LIST OF FIGURES

| | | |
|------|---|----|
| 1.1 | Pictorial depiction of a node x' within the horizon of x | 2 |
| 1.2 | The image shows the path of the crack and the broken bonds. | 2 |
| 1.3 | Nodes that are within a distance δ in both x and y directions of the node at location X | 2 |
| 1.4 | Peridynamic formulation of conduction - Bobaru et al (2010) | 3 |
| 1.5 | Peridynamic formulation of conduction - Bobaru et al (2010)[5] | 4 |
| 2.1 | Peridynamic simulation of a 1 Dimensional rod subjected to 0°C at the left end and 100°C at the right end under steady state conditions.[6] | 6 |
| 2.2 | Contour Plot 2D Steady State Conduction | 6 |
| 2.3 | Mid Plane Temperature 2D Steady State Conduction | 6 |
| 2.4 | Contour Plot 2D Steady State Conduction - Peridynamics | 7 |
| 2.5 | Mid Plane Temperature 2D Steady State Conduction - Peridynamics | 7 |
| 2.6 | The reference result for 2D Plate with central crack in the domain. [7] . . . | 8 |
| 2.7 | Temperature variation in 2D plate in presence of a crack, with 121 nodes. . | 9 |
| 2.8 | Temperature variation in 2D plate in presence of a crack, with 441 nodes. . | 9 |
| 2.9 | Crack growing dynamically along X axis at midway along the Height of plate. | 9 |
| 2.10 | Computational model of quenching by a water jet. | 10 |
| 2.11 | A zoomed in schematic of the surface where water is in contact with it. . . | 10 |
| 2.12 | Temperature profile of plate quenched using water jet | 12 |
| 2.13 | Plate temperature over period of time during quenching. | 13 |
| 2.14 | Comparison between experimental result and simulated result for the time step 735ms. | 13 |

| | | |
|------|--|----|
| 2.15 | Comparison between experimental result and simulated result for the time step 1040ms. | 14 |
| 2.16 | Comparison between experimental result and simulated result for time step 1250ms. | 14 |
| 3.1 | Deformation of the PD material at positions x and x' , with equal and opposing pairwise force densities occurring. | 16 |
| 3.2 | change in shape of 2D plate under mechanical load along y axis | 17 |
| 3.3 | Simulation showing damage (ϕ) in a 2D plate with a hole. | 18 |
| 3.4 | Simulation showing damage (ϕ) in a 2D plate with a crack. | 19 |

Nomenclature

| | |
|-------------|--|
| α | Coefficient of linear expansion ($m/^{\circ}C$) |
| δ | Horizon length (mm) |
| μ | Shear Modulus (Pa) |
| ρ | Density (kg/m^3) |
| ξ_{kj} | Bond length between node j and k (mm) |
| C | Bond constant |
| C_p | Specific heat capacity at constant pressure ($J/Kg.K$) |
| dV_j | Elemental Volume of j^{th} node (mm^3) |
| t | Time (sec) |
| U_k | Displacement of k^{th} node (mm^3) |
| v_c | Volume Correction (mm^3) |
| θ, T | Temperature($^{\circ}C$) |
| DC | Direct Chill (Casting) |
| FFR | Free Falling Region |
| IR | Impingement Region |
| LFP | Leidenfrost Point |
| LFT | Leidenfrost Temperature |
| RR | Radiation Region |

CHAPTER 1

INTRODUCTION

1.1 About Peridynamics

Peridynamics is a non local continuum mechanics formulation developed by Silling [1] [2] [3] to model Crack initiation and propagation.

The classical equations of continuum mechanics cannot be extended specifically when crack surfaces and other singularities are present in a deformation when partial derivatives do not exist. Since they do not include partial derivatives, the integral equations in peridynamic theory can be extended directly[4].

The peridynamic method avoids the need for special fracture mechanics methods by being able to apply the same equations explicitly at all points in a statistical model of a deforming system. A separate crack growth law based on a stress strength factor is not needed in peridynamics, for example.

Main Purpose is to model complex fracture patterns and crack growth.

1.2 Fundamental equation of bond-based Peridynamics

1.2.1 Peridynamics formulation of Mechanics:

The following motion equation is the fundamental equation in peridynamics[2]:

$$\rho \frac{\partial^2 u(x, t)}{\partial t^2} = \int_H f(u(x', t) - u(x, t), x' - x, t) dV_{x'} + b(x, t)$$

x is a point in a body \mathcal{R} , t is time, u is the displacement vector field, and ρ is the mass density in the undeformed body. x' is an integration dummy variable.

The force density that x' exerts on x is represented by the vector valued function f . The relative displacement and relative position vectors between x' and x determine the force density. Force per volume squared is the dimension of f .

A "bond" is the interaction between any x and x' . This interaction's physical mechanism does not need to be defined. When x' is outside a neighborhood of x (in the undeformed configuration) within a certain distance δ called the horizon $H(1)$, it is commonly thought that f vanishes.

The horizon H is mathematically defined as:

$$H = x' \in \text{Re} : |x' - x| < \delta \quad (1)$$

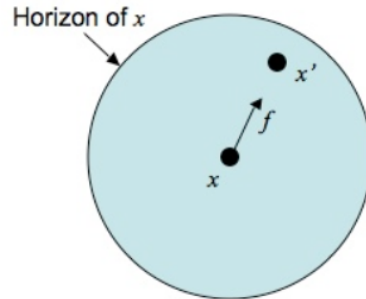


Figure 1.1: Pictorial depiction of a node x' within the horizon of x

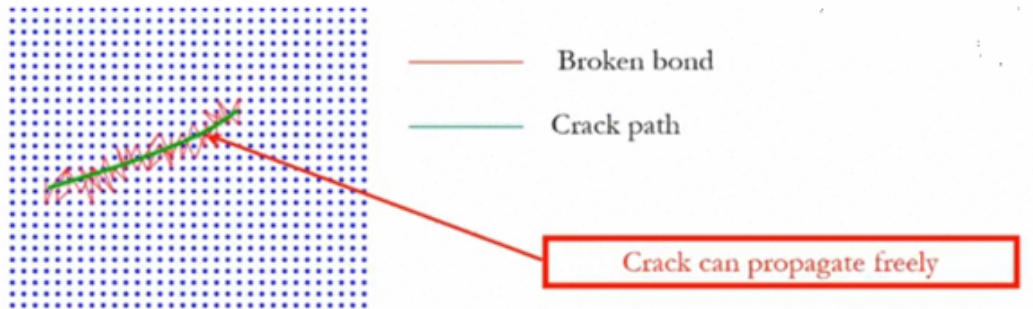


Figure 1.2: The image shows the path of the crack and the broken bonds.

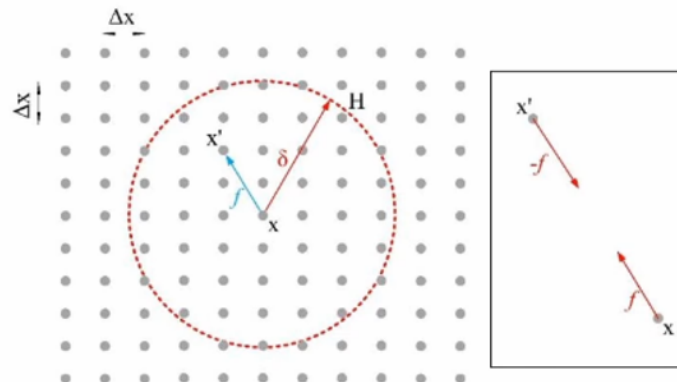


Figure 1.3: Nodes that are within a distance δ in both x and y directions of the node at location X

1.2.2 Peridynamics formulation of Heat Transfer:

- Consider a body occupying a region X (1.2.1) in the three-dimensional space and composed of material points with mass and volume.
- We consider that each material point is connected to the rest of the points in the body X via “thermal bonds” or “t-bonds”.
- Let \vec{e} be a unit vector along the bar.

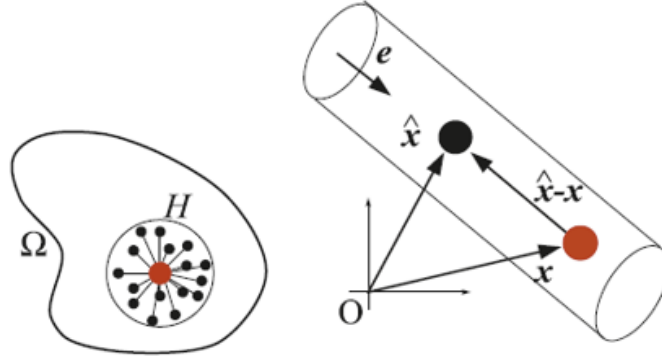


Figure 1.4: Peridynamic formulation of conduction - Bobaru et al (2010)

- The heat is transferred between point x and any point \hat{x} , along the direction of the t-bond vector $\hat{x} - x$.
- It is assumed that interaction distance for every point is limited to a certain region, called horizon H , to be spherical of radius d .

$$\rho C_p (\hat{x} - x) \cdot e \frac{\partial \theta_a(x, \hat{x}, t)}{\partial t} = K(\hat{x}, x) \cdot \frac{\theta(\hat{x}, t) - \theta(x, t)}{(\hat{x} - x) \cdot e} \quad (2)$$

- Now divide by $(\hat{x} - x)$ on both sides, and integrate it over the horizon.

$$\int_{H_x} \rho C_p \frac{\partial \theta_a(x, \hat{x}, t)}{\partial t} d\hat{x} = \int_{H_x} K(x, \hat{x}) \cdot \frac{\theta(\hat{x}, t) - \theta(x, t)}{||(\hat{x} - x)||^2 \cdot e} d\hat{x} \quad (3)$$

- The average temperatures in all the t-bonds connecting at x are assumed to obey the following relationship between the temperature at point x and time t :

$$\int_{H_x} \rho C_p \theta_a(x, \hat{x}, t) d\hat{x} = \rho C_p \theta(x, t) V_{H_x} \quad (4)$$

and subsequently,

$$\int_{H_x} \rho C_p \frac{\partial \theta_a(x, \hat{x}, t)}{\partial t} d\hat{x} = \rho C_p \frac{\partial \theta(x, t)}{\partial t} V_{H_x} \quad (5)$$

The final equation will now become,

$$\rho C_p \frac{\partial \theta(x, t)}{\partial t} V_{H_x} = \int_{H_x} k(x, \hat{x}) \cdot \frac{\theta(\hat{x}, t) - \theta(x, t)}{\|(\hat{x} - x)\|^2 \cdot e} d\hat{x} = \int_{H_x} \Theta(x, \hat{x}, \theta(x, t), \theta(\hat{x}, t), t) d\hat{x} \quad (6)$$

where $k(x, \hat{x}) = K(x, \hat{x})/V_{H_x}$, which is named as *micro-conductivity* of the t-bond (x, \hat{x}) .

This above equation can be extended for 2D and 3D as well.

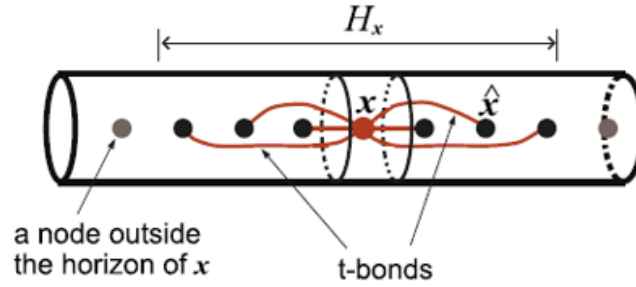


Figure 1.5: Peridynamic formulation of conduction - Bobaru et al (2010)[5]

1.3 Need for a new computational model

- Simulating crack propagation is extremely challenging task.
- Most widely used method for simulation is Finite Element Method. It has two major disadvantages.
 - Crack always propagate along element boundaries.
 - Re-meshing is need to be done for cracking.

$$\rho \ddot{u} = \nabla \cdot \sigma(x, t) + b(x, t) \quad (7)$$

vs

$$\rho \ddot{u} = \int_H f(u - u, x' - x, t) dV_{x'} + b(x, t) \quad (8)$$

As the peridynamic governing equations utilise integral expressions (7) as compared to differential terms (8) in classical formulation, peridyanmic theory remains valid to simulate displacement fields even in the presence of discontinuities such as cracks.

CHAPTER 2

Peridynamic Formulation for simulating Thermal Effects

2.1 1D Steady State Conduction

2.1.1 Analytical Solution:

The analytical solution for the temperature profile in the material for Heat Conduction is the solution to the Euler's Heat Conduction equation,

$$\nabla^2 T + \frac{s_{gen}}{k} = \frac{\rho C_p}{k} \frac{\partial T}{\partial t} \quad (9)$$

Reducing (9) for the 1D Steady State Case with no internal heat generation, we get,

$$\frac{d^2 T}{dx^2} = 0 \quad (10)$$

The solution to (10) is a straight line. For a 1D Rod subjected to different temperatures on either end of the rod, the temperature profile is a straight line connecting the Temperatures at the either end of the rod.

2.1.2 Peridynamic Simulation:

| | |
|---------------------|---|
| Boundary Condition: | T(left wall) = 0 °C, T(right wall) = 100 °C |
| Rod dimensions: | Length = 10 cm |

Simulation for Temperature Profile in the case of a 10 cm rod approximated as a 1D element and subjected to a left end temperature of 0 °C and right end temperature of 100 °C was simulated in Matlab using the peridynamics conduction formulation. The solution obtained is a straight line between 0 °C and 100 °C with small deviations near the ends of the rods as seen in Fig [2.1].

Thus, the simulation agrees closely with the expected analytical result. The deviation near the ends is due to surface effects that has not been considered in this simulation. However, corrections for the surface effects has been included in further simulations.

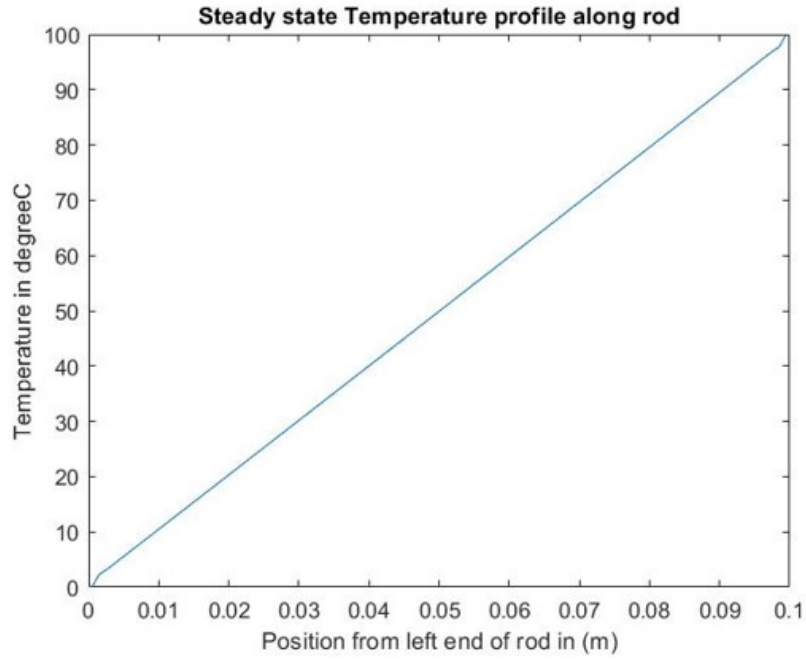


Figure 2.1: Peridynamic simulation of a 1 Dimensional rod subjected to 0°C at the left end and 100°C at the right end under steady state conditions.[6]

2.2 2D Steady State Conduction

2.2.1 Analytical Solution:

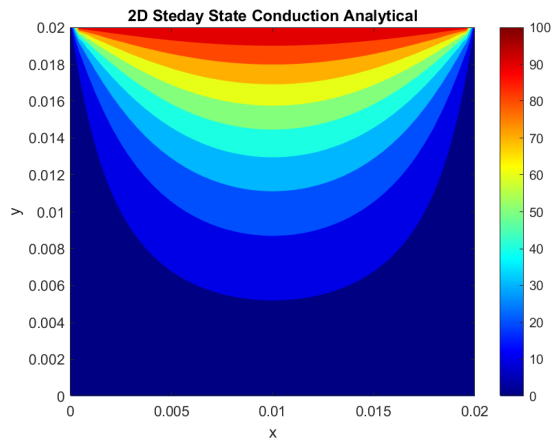


Figure 2.2: Contour Plot 2D Steady State Conduction

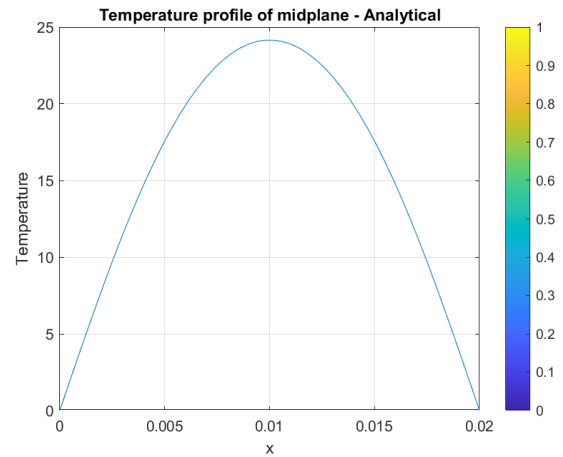


Figure 2.3: Mid Plane Temperature 2D Steady State Conduction

2.2.2 Peridynamic Solution:

| | |
|-----------------------------|--|
| Initial Condition: | $T(x,y) = 0\text{ }^{\circ}\text{C}$ |
| Boundary Condition: | $T(\text{top wall}) = 100\text{ }^{\circ}\text{C}$ |
| Aluminium Plate dimensions: | Length = 2cm, Height = 2cm, Thickness = 0.01 cm |

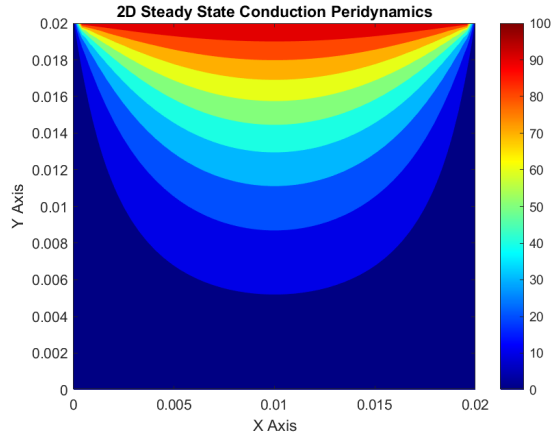


Figure 2.4: Contour Plot 2D Steady State Conduction - Peridynamics

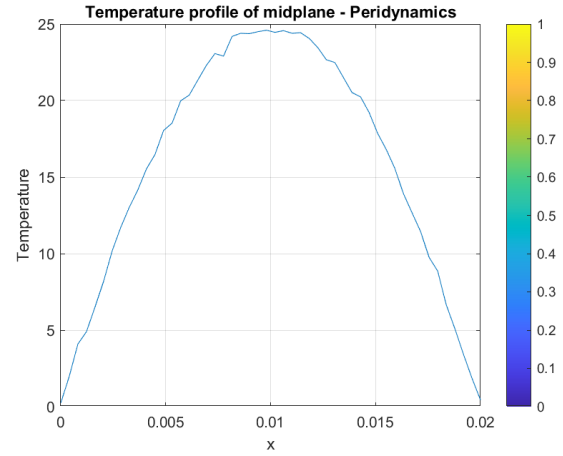


Figure 2.5: Mid Plane Temperature 2D Steady State Conduction - Peridynamics

- As seen from analytical and peridynamic contour plots and temperatures, there is close agreement between the analytical and peridynamic solutions.
- The variations near the ends of the plate is due to **end effects** which can be overcome by creating a fictitious material layer extending the plate boundary to compensate for the lesser node interactions near the ends.

2.3 2D Transient Conduction profile with crack in domain

2.3.1 Problem definition :

| | |
|-----------------------------|---|
| Initial Condition: | $T(x,y) = 500\text{ }^{\circ}\text{C}$ |
| Boundary Condition: | $T(\text{bottom wall}) = -100\text{ }^{\circ}\text{C}$, $T(\text{top wall}) = 100\text{ }^{\circ}\text{C}$ |
| Aluminium Plate dimensions: | Length = 2cm, Height = 2cm, Thickness = 0.01 cm |
| Crack dimensions: | Length = 1cm, from (0.5,1) to (1.5,1) |

- In-order to simulate transient conduction in material with cracks, a simulation was performed with a simple case of 2D plate with a predefined crack subjected to boundary conditions as mentioned above and the thermal profile was analysed.
- From the graph in the reference Fig [2.6], we can infer that the temperature is rising as we move along the y axis from $-100\text{ }^{\circ}\text{C}$ to $100\text{ }^{\circ}\text{C}$ but remains constant in the crack region. This trend is also observed in the peridynamic simulation as seen in Fig [2.7] and Fig [2.8].
- This is because the interactions between nodes which have crack in between them are not considered due to the presence of crack. Hence there is a less effective heat transfer as compared to the case where there is no crack.

- The reason why the length and height of the specimen split in of odd numbers is to ensure that nodes do not lie directly on the cracks.
- If the node is on the crack, that node should be removed and we should re-mesh. Hence we tried two cases, one with 121 nodes and another with 441 nodes, (i.e) splitting the length and height into 11 parts and 21 parts respectively.

The reference result [7] for this problem is as follows :

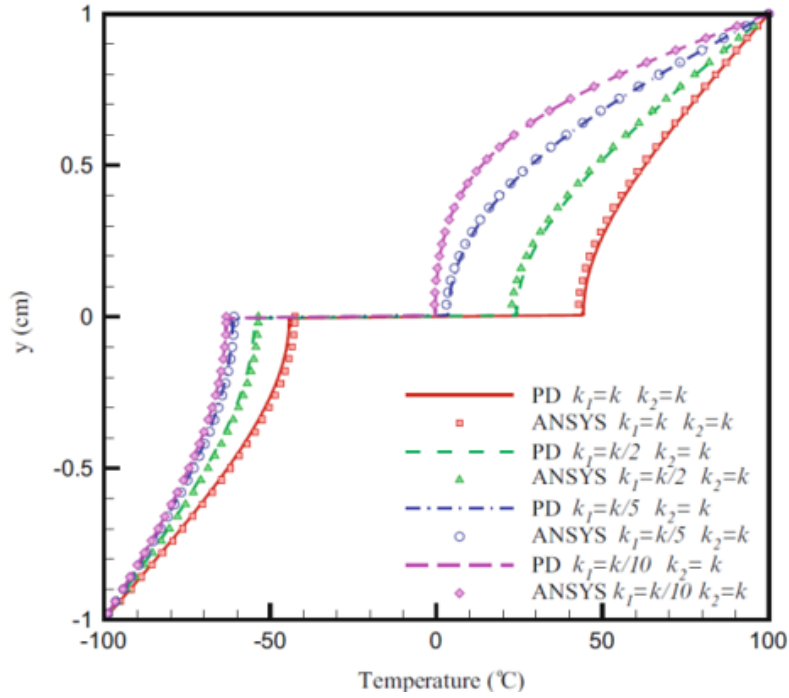


Figure 2.6: The reference result for 2D Plate with central crack in the domain. [7]

2.3.2 Effect on increasing number of nodes:

- We can see that 441 nodes temperature profile is more towards the reference result than the 121 nodes temperature profile. We get accurate results when number of nodes are increased. This can be seen from Fig [2.7] and Fig [2.8].
- However, increasing the number of nodes also increases the computational power required for the simulation and hence it is not computed in this work.

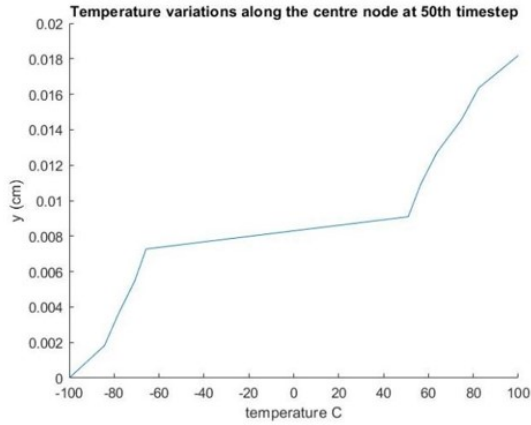


Figure 2.7: Temperature variation in 2D plate in presence of a crack, with 121 nodes.

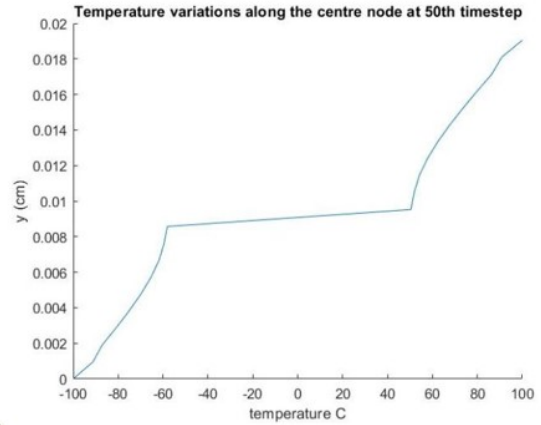


Figure 2.8: Temperature variation in 2D plate in presence of a crack, with 441 nodes.

2.4 Crack propagation without mechanical coupling

| | |
|-----------------------------|---|
| Initial Condition: | $T(x,y) = 500\text{ }^{\circ}\text{C}$ |
| Boundary Condition: | $T(\text{bottom wall}) = -100\text{ }^{\circ}\text{C}$, $T(\text{top wall}) = 100\text{ }^{\circ}\text{C}$ |
| Aluminium Plate dimensions: | Length = 2cm, Height = 2cm, Thickness = 0.01 cm |
| Crack dimensions: | Length = $0.025 * t$ cm, where 0.025 is the crack propagation speed. |

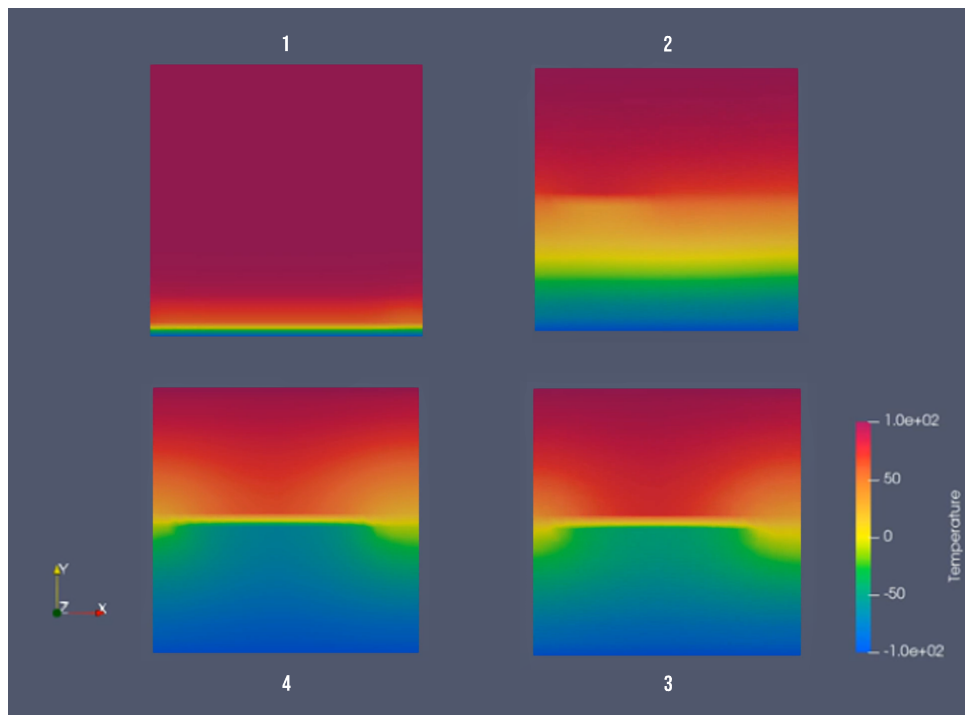


Figure 2.9: Crack growing dynamically along X axis at midway along the Height of plate.

- Simulation for the crack growth only using temperature changes without mechanical coupling (to simulate system dynamics) was carried out.
- The simulation was able to accommodate the dynamically changing crack and account for the changes and predict the temperature profile.

2.5 Metal Quenching in Direct Chill Casting Process

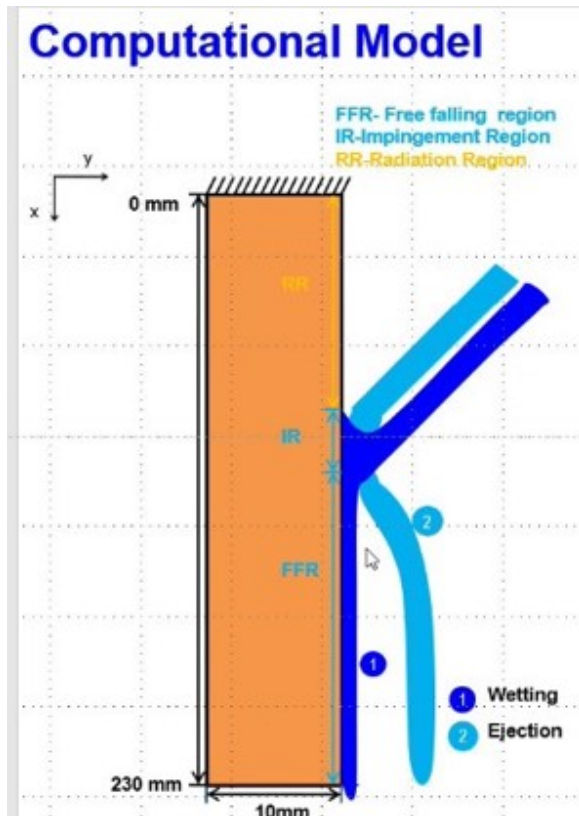


Figure 2.10: Computational model of quenching by a water jet.

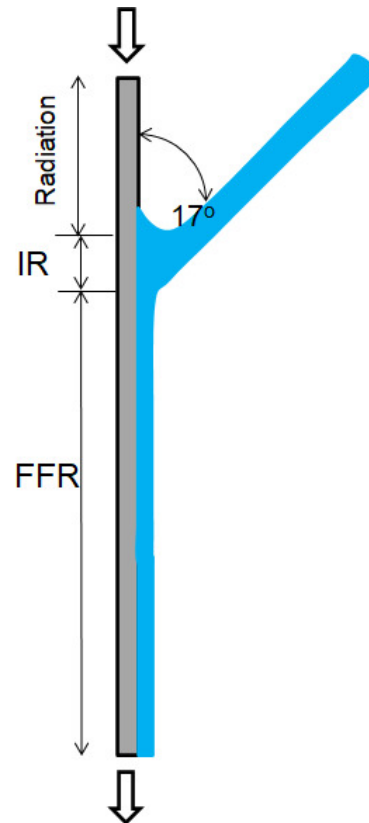


Figure 2.11: A zoomed in schematic of the surface where water is in contact with it.

The semi-continuous direct chill (DC) casting process is one of the primary technology used to cast sheet ingots [8]. The most critical stage of the DC casting process is the quenching process as a number of defects can arise including hot tears, cold shuts, cracks, and in extreme cases, hang-up and breakouts. The rate of heat transfer to the cooling medium is usually described by a boiling curve [9], which relates the rate of heat extraction (heat transfer coefficient or heat flux) to surface temperature.

The flow if water over the ingot for cooling process undergoes a film boiling process. In the presence of film boiling, heat transfer becomes more complicated as a portion of the water may be ejected from the ingot surface.

During water ejection as seen in Fig [2.10], the heat transfer rate is significantly lower below the point of water ejection, as there is little or no contact of the water curtain with the ingot surface. The stable film layer then gradually collapses as the casting proceeds and water flow rates are increased. The extent of film boiling can influence the thermal profile in the ingot base leading to the formation of local hot spots and subsurface cracks (hot tears).

As a computational model, the billet is approximated as a 2D Plate, and the water falls on the right end of the plate as shown in Fig [2.10] and Fig [2.11].

During unsteady behaviour (as in the case of quenching process), where the temperature at the impingement point is varying with time, each point on the surface of the casting is assigned its own unique boiling curve, dependent on the impingement point temperature experienced by that point on the ingot surface.

In the implementation subroutine, the temperature at every stream position (as determined at the material integration points for every element on the vertical ingot surface) is compared with the Leidenfrost temperature (i.e. the temperature above which film boiling heat transfer is predominant) at the beginning of every time increment. If at a certain stream position, the temperature exceeds the Leidenfrost temperature, all the stream positions below it are assigned a lower heat transfer coefficient of approximately $200 \text{ W/m}^2/\text{K}$, to simulate reduced heat transfer associated with the ejection of water. All the stream positions above it are cooled as per the boiling curve.

2.5.1 Peridynamics Results:

| | |
|--|--|
| Plate dimensions: | Width = 200 cm, Height = 100 cm, Thickness = 1 cm |
| Density | 2600 kg m^{-3} |
| C_p | $1000 \text{ J kg}^{-1} \text{ K}^{-1}$ |
| k_{macro} | 200 S m^{-1} |
| Jet velocity | 10 mm s^{-1} |
| Volume flowrate | $10 \text{ l m}^{-1} \text{ min}^{-1}$ |
| Temperature of cooling water | 50 °C |
| Ambient Temperature | 50 °C |
| Max Heat Flux | $7 \times 10^6 \text{ W/m}^2$ |
| Nucleate Boiling Temperature | 180 °C |
| Leidenfrost Temperature | 500 °C |
| Leidenfrost Heat Flux | $\frac{\text{Max Heat Flux}}{2}$ |
| Crack Positions from the left end (cm) | crack1 = 56, crack2 = 87.111, crack3 = 107.556 crack4 = 125.333, crack5 = 168.889, crack6 = 142.222 |

The thermal profile of a moving plate with the above specifications was simulated.

- A Peridynamic simulation was carried out for 14 seconds and the following temperature profiles as in Fig [2.12] were obtained.
- As expected the temperatures are discontinuous near the crack. Since this is a cooling process we expect sudden temp drop near the crack.

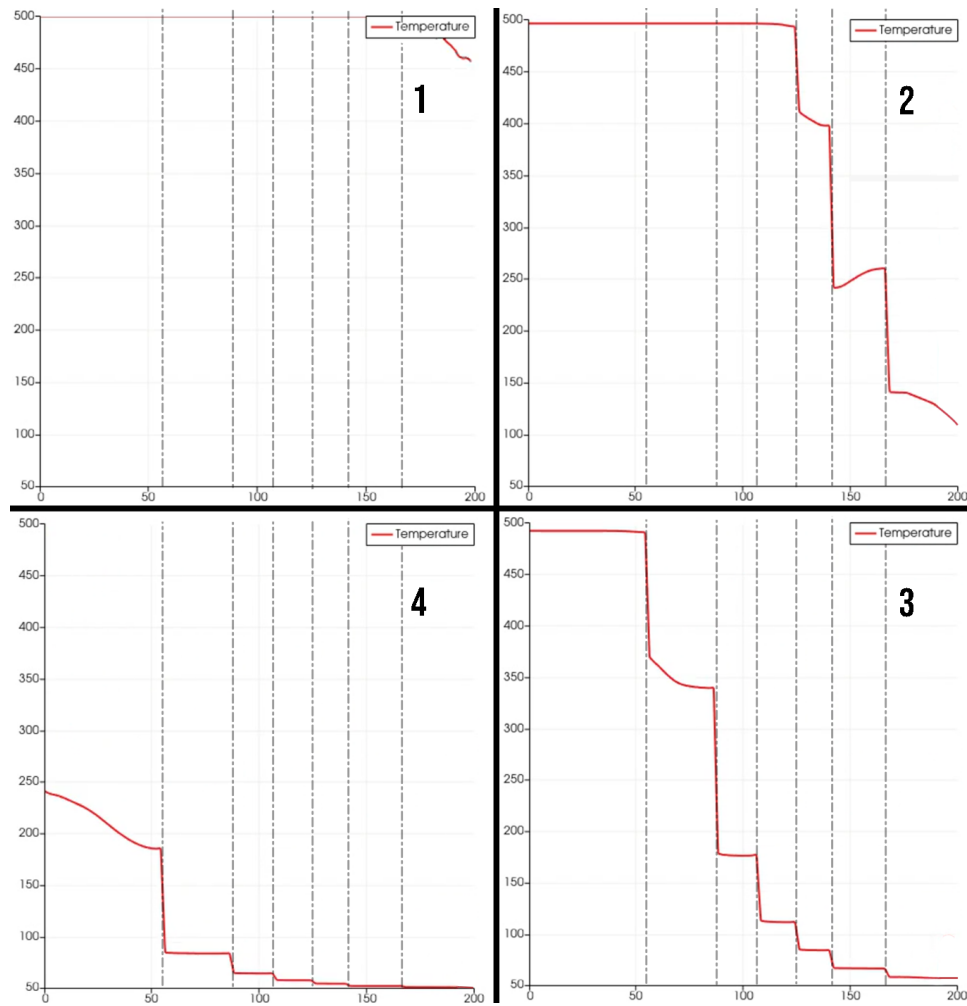


Figure 2.12: Temperature profile of plate quenched using water jet

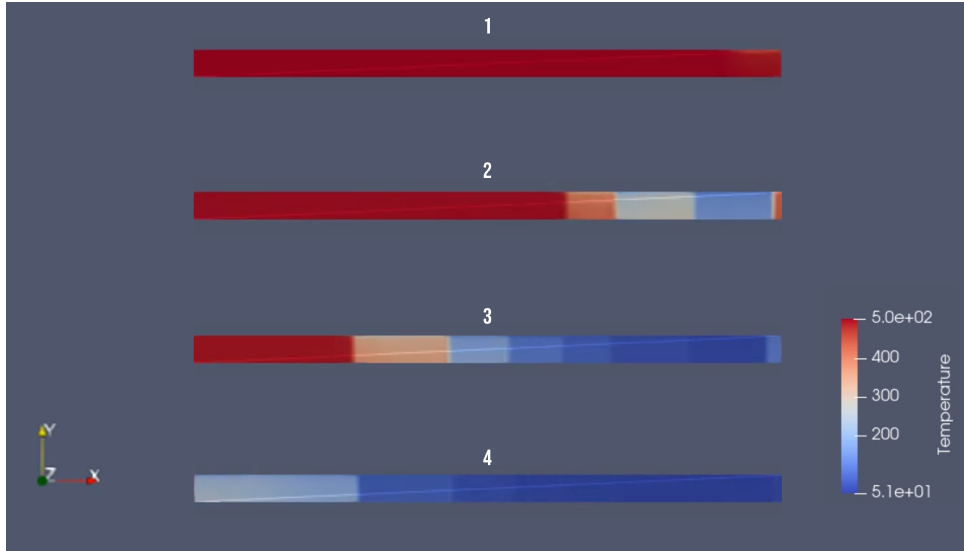


Figure 2.13: Plate temperature over period of time during quenching.

2.5.2 Comparison

- The trend in the peridynamic model is seen to follow the trend from the experimental results.
- There is a drop in temperature near the crack regions as expected. However refinement of model required to achieve accurate results.

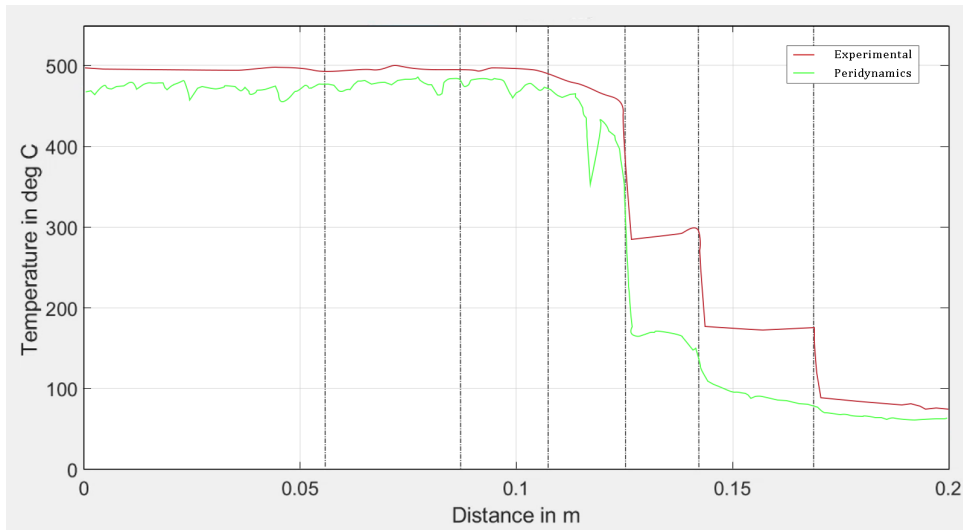


Figure 2.14: Comparison between experimental result and simulated result for the time step 735ms.

- Initially as seen in Fig [2.14], there is a disagreement between the experimental and peridynamic results. This may be due to end effects and can be rectified by extension of the horizon beyond the material boundaries to include more material interactions.

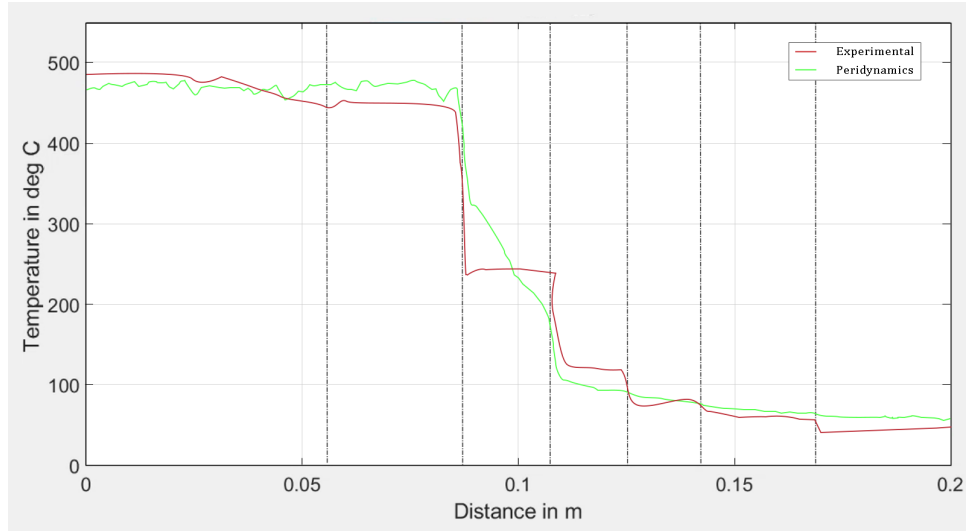


Figure 2.15: Comparison between experimental result and simulated result for the time step 1040ms.

- As seen in Fig [2.15], there is a slight disagreement between the experimental and peridynamic results between 0.08 m and 0.12 m. However, the trend is followed by the simulation data and sharp discontinuities through temperature drops are obtained near crack boundaries.

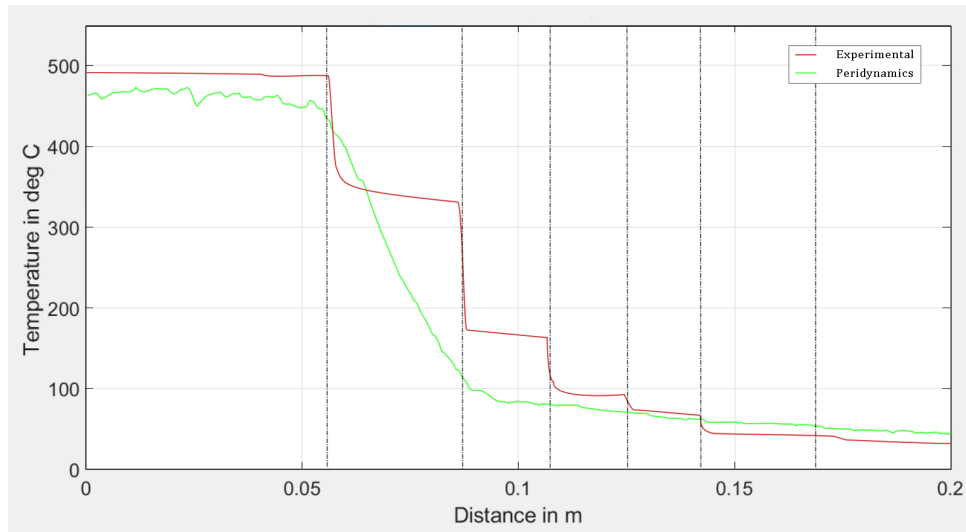


Figure 2.16: Comparison between experimental result and simulated result for time step 1250ms.

- There is a disagreement between the simulated results and experimental results as seen in Fig [2.16] in the region between 0.05 m and 0.08 m. This maybe due to dynamic crack growth. Thermo-mechanical coupling should be implemented to verify this argument.

CHAPTER 3

Peridynamic Formulation for simulating Mechanical Effects

3.1 Mechanical damage formulation

Material point x interacts with its family of material points and is conditioned by their mutual deformation. Similarly, deformation of the material points influences material point x' of its own family. The content points x and x' undergo displacements, u and u' , respectively, in the deformed configuration, as seen in Fig [3.1]. Prior to deformation, their original relative position vector $(x' - x)$ becomes $(y' - y)$ after deformation. Here force density vector f is defined as force vector per unit volume squared that the material exerts force among nodes y to y' and vice versa, and is referred as the pairwise response function [10] . The distance between material points x and x' is known as the stretch s , and it is defined as [11]

$$s(u' - u, x' - x) = \frac{|y' - y| - |x' - x|}{|x' - x|} \quad (11)$$

When this stretch s exceed critical stretch s_0 (12) bond between the nodes break. This breaking of bond leads to crack at a macro scale.

$$s_0 = \sqrt{\frac{10G_0}{\pi c \delta^5}} = \sqrt{\frac{5G_0}{9k\delta}} \quad (12)$$

where, G_0 is the fracture energy of the material.

The bond constant c can be expressed as,

$$c = \frac{24\mu}{\pi t \delta^3} = \frac{12K}{\pi t \delta^3} \quad (13)$$

here t refers to thickness of the plate, K is bulk modulus and μ is shear modulus

The bond failure criterion[12] is introduced as:

$$\mu(t, x' - x) = \begin{cases} 1, & \text{if } s(t', x' - x) < s_0 \text{ for all } 0 \leq t' \leq t \\ 0, & \text{otherwise} \end{cases}$$

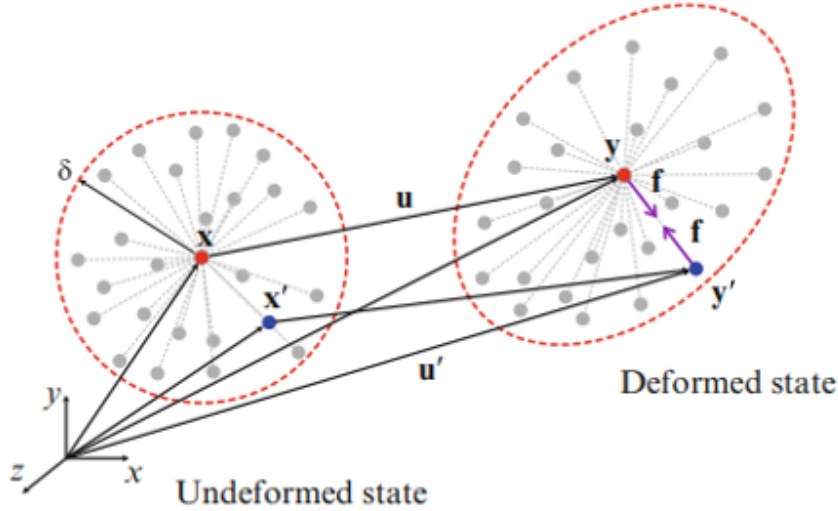


Figure 3.1: Deformation of the PD material at positions x and x' , with equal and opposing pairwise force densities occurring.

ϕ is used to describe the local damage degree of a single material point, can be found from the below equation

$$\phi = 1 - \frac{\int \mu(x - x', t) dV'}{\int dV'} \quad (14)$$

3.2 2D Plate subjected to Mechanical displacement

| | |
|-----------------------------|---|
| Boundary Condition: | $u(\text{top wall}) = 0.1 \text{ cm}$ |
| Aluminium Plate dimensions: | Length = 2cm, Height = 2cm, Thickness = 0.01 cm |
| Number of nodes: | 10,000 |
| Horizon: | $4 * dx (= 0.02 \text{ cm})$ |

- In-order to simulate mechanical loading on materials, a simple case of a 2D plate was taken and the changes to the plate when subjected to uni-axial loading along Y axis was observed.
- This simulation shows the displacement in the nodes when subjected to a displacement boundary condition of 1cm on the top layer of the plate.
- The Figure [3.2] shows the change in shape of the plate when subjected to a uni-axial mechanical loading along the Y axis. The first image labeled 1 in Fig [3.2] is the initial shape of the plate and the second image labeled 2 in Fig [3.2] shows the deformed plate after loading.

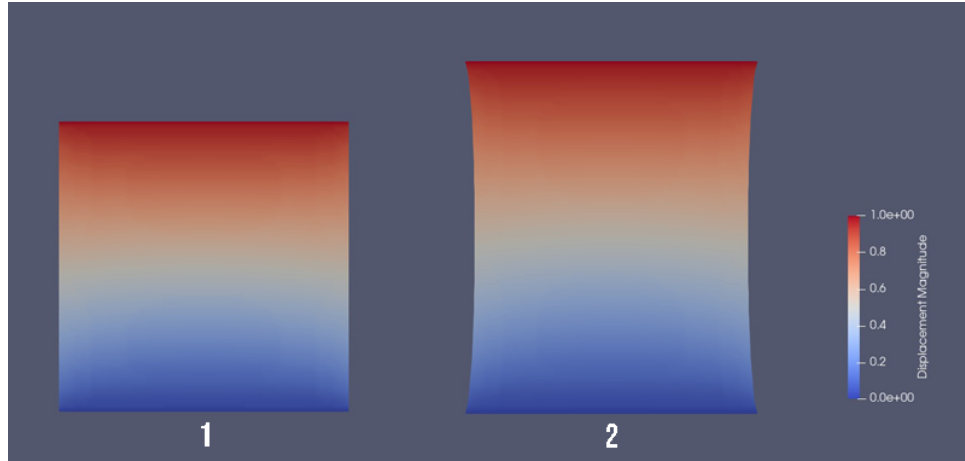


Figure 3.2: change in shape of 2D plate under mechanical load along y axis

- **When subjected to a loading only along the Y axis, poisson's ratio effect can also be seen and displacement is seen (but scaled down by the poisson's ratio) along the X axis as well.**
- A more accurate result can also be obtained by increasing the number of nodes. We have used 10,000 nodes but increasing the number of nodes to 1,00,000 makes it computationally intensive as peridynamic formulation takes into account all nearby interactions within the horizon.

3.3 2D Plate with hole subjected to Mechanical Displacement

| | |
|-----------------------------|---|
| Boundary Condition: | $u(\text{top wall}) = 0.1 \text{ cm}$ |
| Aluminium Plate dimensions: | Length = 2cm, Height = 2cm, Thickness = 0.01 cm |
| Hole dimensions: | circle with radius = 4mm and center (1,1) |
| Number of nodes: | 10,000 |
| Horizon: | $4 * dx (= 0.02 \text{ cm})$ |

- In-order to simulate hollow materials, a simple case of a 2D plate with a central internal hole was taken and the changes to the plate when subjected to uni-axial loading along Y axis was observed.
- The simulation was carried out to compute the displacement in the nodes when subjected to a displacement boundary condition of 1cm on the top layer of the plate.
- The Fig [3.4] depicts a scalar value called damage (which is a measure of the probability of the bond breakage and hence crack formation) in the 2D aluminium plate when the loading is applied on the top layer of the plate.

- As expected, there is a high chance of crack formation near the edges of the hole boundaries. When subjected to a loading only along the Y axis, poisson's ratio effect can also be seen and damage is obtained (but scaled down by the poisson's ratio) along the X axis as well.
- The displacements has been scaled by a factor of 10, to make the displacement and damage to the bonds more visible.
- A more accurate result can also be obtained by increasing the number of nodes. We have used 10,000 nodes but increasing the number of nodes to 1,00,000 makes it computationally intensive as peridynamic formulation takes into account all nearby interactions within the horizon.

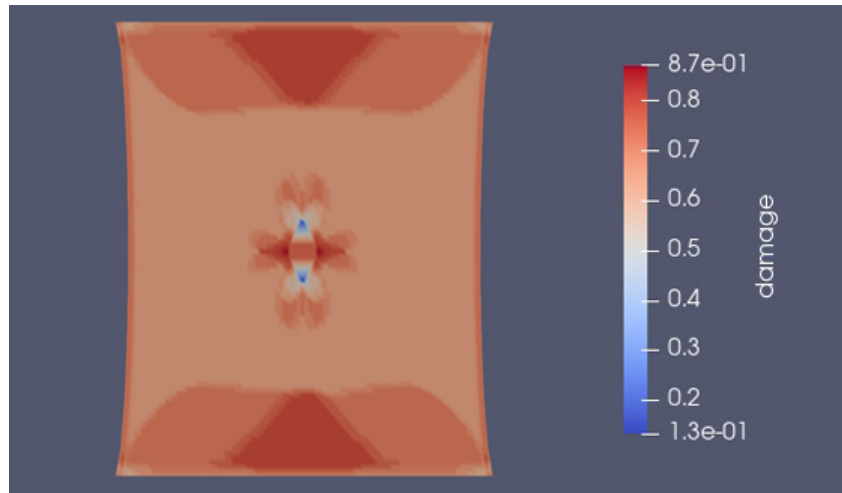


Figure 3.3: Simulation showing damage (ϕ) in a 2D plate with a hole.

- As seen in the Fig [3.4], there is damage near the top layer and bottom layers of the plate. This is due to non-incorporation of end effects which requires the extension of the peridynamic horizon near the plate boundary to 2 or 3 times beyond the dimensions of the plate.
- When these end effects are implemented in the code, these abnormalities can be removed.

3.4 2D Plate with crack subjected to Mechanical Displacement

| | |
|-----------------------------|---|
| Boundary Condition: | $u(\text{top wall}) = 0.1 \text{ cm}$ |
| Aluminium Plate dimensions: | Length = 2cm, Height = 2cm, Thickness = 0.01 cm |
| Crack dimensions: | Length = 1cm, from (0.5,1) to (1.5,1) |
| Number of nodes: | 10,000 |
| Horizon: | $4 * dx (= 0.02 \text{ cm})$ |

- In-order to simulate material discontinuities i.e cracks, a simple case of a 2D plate with a horizontal predefined crack was taken and the changes to the plate when subjected to uni-axial loading along Y axis was observed.
- The simulation was carried out to compute the displacement in the nodes when subjected to a displacement boundary condition of 0.1 cm on the top layer of the plate.
- The Fig [3.4] depicts a scalar value called damage (which is a measure of the probability of the bond breakage and hence crack formation) in the 2D aluminium plate when the loading is applied on the top layer of the plate.
- As expected, **there is a high chance of crack formation near the edges of the crack boundaries. When subjected to a loading only along the Y axis, poisson's ratio effect can also be seen and damage is obtained (but scaled down by the poisson's ratio) along the X axis as well.**
- The displacements has been scaled by a factor of 10, to make the displacement and damage to the bonds more visible.
- A more accurate result can also be obtained by increasing the number of nodes. We have used 10,000 nodes but increasing the number of nodes to 1,00,000 makes it computationally intensive as peridynamic formulation takes into account all nearby interactions within the horizon.

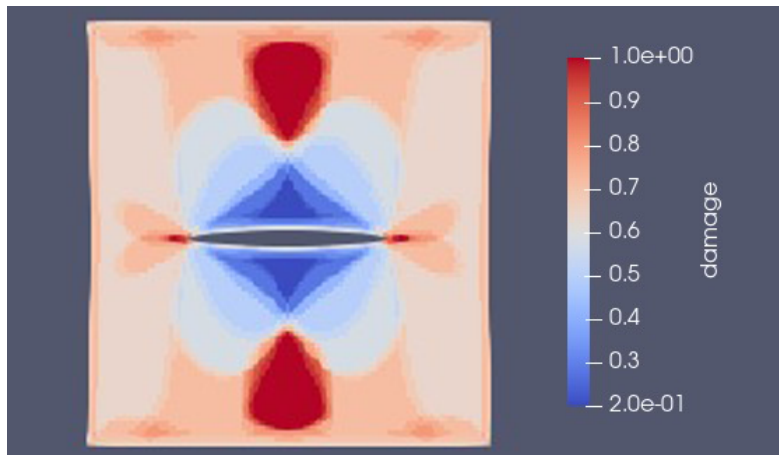


Figure 3.4: Simulation showing damage (ϕ) in a 2D plate with a crack.

- As seen in Fig [3.4], there is damage near the top layer and bottom layers of the plate. This is due to non-incorporation of end effects which requires the extension of the peridynamic horizon near the plate boundary to 2 or 3 times beyond the dimensions of the plate. When these end effects are implemented in the code, these abnormalities can be removed.

CHAPTER 4

Conclusion and Scope for future Work

4.1 Conclusion

Bond Based peridynamics Approach has been used to simulate various thermo-mechanical effects in this work and the following can be concluded:

- Bond based Peridynamics is restricted to materials with Poisson ratio of 0.3. Since most of the engineering materials have a poisson ratio of 0.3, this is a sufficient approximation for the dynamics.
- In order to simulate for general materials, a state based approach should be used. (Bond based peridynamics is a special case of state based peridynamics).
- Peridynamics formulation agrees with the results obtained from other numerical methods like FEM, FDM and FVM and also with the analytical solutions when simulated with more refined meshes. However, peridynamics approach requires more computation power compared to other traditional numerical methods.
- Peridynamics can simulate crack origination, evolution and propagation easier than other methods (irrespective of discontinuities) but there is a trade-off in computational power as peridynamics involves more interaction computations.

4.2 Future Work

- State Based peridynamic approaches must be implemented to simulate materials with poisson's ratio other than 0.3. Simulation for materials other than steel and aluminium like porous media which has many engineering applications needs state based formulations. State based formulation methods must be developed to simulate a wide range of engineering materials.
- In this work thermal and mechanical formulation of peridynamics has been performed independently but coupling of the the individual effects to simulate crack dynamics like crack growth and propagation has not been performed. Implementation of coupled effects needs to be done to simulate practical material failure cases.

APPENDIX A

Peridynamics - Matlab Implementation

A.1 Peridynamics Simulation Overview

The development of solution algorithm from the peridynamic equation of the motion may involve the following steps:

1. Initiate the matrices and provide the input parameters.
2. For the temporal integration, determine a stable time step size. The time step size is equal to 1 if the analysis uses the adaptive dynamic relaxation methodology.
3. Generate the material points.
4. Calculate and save the material points inside each material point's horizon.
5. Remove any peridynamic interactions that are passing through the crack surfaces if a pre-existing crack issue exists.
6. For each material point, determine the surface correction factor.
7. Apply the initial conditions.
8. Construct the stable mass matrix if the analysis involves adaptive dynamic relaxation technique.
9. Begin time integration.
10. Boundary conditions should be applied.
11. Calculate the total peridynamic interaction forces that each material (collocation) point is subjected to.
12. If the stretch of the peridynamic interaction surpasses the critical stretch, it must be terminated.
13. Compute the adaptive dynamic relaxation technique parameters if it's used in the analysis.
14. To get displacements and velocities, time integration is used.

A.2 Volume Correction for Interactions:

The peridynamic equation of motion is an integro-differential equation that is hard to resolve analytically. As a result, computational methods for spatial and time integrations are used to establish the solution. The collocation approach of a meshless scheme can be used to perform spatial integration due to its simplicity. As a result, the domain can be divided into a finite number of subdomains, each with its own set of integration or collocation points.

However, each substance point's volume can not be fully embedded in the horizon, resulting in truncated volumes near the horizon's surface. As a consequence, if the entire volume of each material point is used in the numerical implementation, the volume integration over the horizon could be erroneous. To compensate for the additional volume, a volume correction factor is required.

```

1 % Initialize variables to speed up calculations
2 volume_correction = zeros(total_number_of_interactions,1);
3 distance_of_interaction = zeros(total_number_of_interactions,1);
4
5 % Loop through every interaction
6 for interaction = 1 : total_number_of_interactions
7
8     % Get position of node
9     node_position = domain(interaction_id(interaction,1),:);
10
11    % Get position of neighbour node
12    neighbour_position = domain(interaction_id(interaction,2),:);
13
14    % Calculate the bond distance
15    distance = norm(node_position - neighbour_position);
16
17    % Calculate the volume correction for the interaction
18    if distance >= horizon_length - r && distance <= horizon_length
19        volume_correction(interaction) = (horizon_length + ...
20            r - distance)/2/r;
21    else
22        volume_correction(interaction) = 1;
23    end
24
25    distance_of_interaction(interaction) = distance;
26
27 end

```

Listing A.1: Volume Correction Implementation Code

A.3 Surface Correction for Interactions:

```

1 surface_correction = zeros(total_number_of_interactions,1);
2 counter = 1;
3 Temp_to_compute_surface_correction = zeros(length(domain),1);
4
5 for i = 1 : length(domain)
6     LT = domain(i,:);
7     Temp_to_compute_surface_correction(counter) = sum(LT);
8     counter = counter + 1;
9 end
10
11 Z_k = zeros(length(domain),1);
12 Z_classical = ones(length(domain),1) * material_macro_thermal_conductivity;
13
14 for interaction = 1 : total_number_of_interactions
15     Lid = interaction_id(interaction,:);
16     current_node = Lid(2);
17     neighbour_node = Lid(1);
18
19     Z_k(current_node) = Z_k(current_node) + .5*.5*
        micro_thermal_conductivity*...

```



```

20     (Temp_to_compute_surface_correction(neighbour_node)-
21     Temp_to_compute_surface_correction(current_node))...
21     ^2*volume_correction(interaction) * elemental_volume/
22     distance_of_interaction(interaction); % Eq.12.90 &, 12.56, 12.53
22 end
23
24 Nodal_surf_corr = Z_classical ./ Z_k;
25
26 for interaction = 1 : total_number_of_interactions
27     Lid = interaction_id(interaction,:);
28     current_node = Lid(2);
29     neighbour_node = Lid(1);
30
31     surface_correction(interaction) = .5 * (Nodal_surf_corr(current_node) +
32     Nodal_surf_corr(neighbour_node));
32 end

```

Listing A.2: Surface Correction Implementation Code

A.4 Remove Interactions crossing Crack:

This function is used to create a flag cell to include/neglect the interaction:

- Consider the crack initial position vector as \vec{a} and the crack end position as \vec{b} . The line equation in vector form of the 2 points \vec{a} and \vec{b} is given by $\vec{r} = \vec{a} + k(\vec{b} - \vec{a})$ where $k \in \mathbb{R}$.
- Consider the current node position vector as \vec{p} and the interaction node neighbour position vector as \vec{q} . The line equation in vector form of the 2 points \vec{p} and \vec{q} is given by $\vec{r} = \vec{p} + t(\vec{q} - \vec{p})$ where $t \in \mathbb{R}$.
- The point of intersection of the two lines can be found by equating the for both the lines i.e. $\vec{p} + t(\vec{q} - \vec{p}) = \vec{a} + k(\vec{b} - \vec{a})$.
- Since there are 2 unknowns, in order to eliminate one of the equations, taking cross product of $(\vec{q} - \vec{p})$ on both sides eliminates t .
- Similarly, taking cross product of $(\vec{b} - \vec{a})$ on both sides eliminates k . The point of intersection lies in between the lines if and only if $0 \leq k \leq 1$ and $0 \leq t \leq 1$.

```

1 function [interaction_crossing_crack_flag_vector] =
2 find_interactions_crossing_crack_in_domain(domain, ...
3 interaction_id , crack_starting_point , crack_ending_point)
4
5 % Line equation of crack in vector form a + t (b-a) where a,b are two
6 % points
7 a = crack_starting_point;
8
9 % b is the endpoint of the crack
10 b_minus_a = crack_ending_point - crack_starting_point;
11
12 % Initialize variable to speed up calculations
13 interaction_crossing_crack_flag_vector = zeros(length(interaction_id)
14 ,1);

```

```

13  for interaction = 1 : length(interaction_id)
14      point1 = [domain(interaction_id(interaction,2),1), domain(
15                  interaction_id(interaction,2),2)];
16
17      point2 = [domain(interaction_id(interaction,1),1), domain(
18                  interaction_id(interaction,1),2)];
19
20      % Line equation of line joining current node (q) and neighbour (s)
21      s = point2 - point1;
22
23      k = (compute_cross_product(a,b_minus_a) - compute_cross_product(
24          point1, b_minus_a))/compute_cross_product(s,b_minus_a);
25
26      t = (compute_cross_product(point1,s) - compute_cross_product(a,s))/
27          compute_cross_product(b_minus_a,s);
28
29      if and(and(t >= 0, t <= 1), and(k >= 0, k <= 1))
30          interaction_crossing_crack_flag_vector(interaction) = 0;
31      else
32          interaction_crossing_crack_flag_vector(interaction) = 1;
33      end
34  end
35 end

```

Listing A.3: Remove interactions crossing crack Implementation Code

REFERENCES

- [1] “Reformulation of elasticity theory for discontinuities and long-range forces”. In: *Journal of the Mechanics and Physics of Solids* 48.1 (2000), pp. 175–209. ISSN: 0022-5096. DOI: [https://doi.org/10.1016/S0022-5096\(99\)00029-0](https://doi.org/10.1016/S0022-5096(99)00029-0).
- [2] Stewart A Silling, Markus Zimmermann, and Rohan Abeyaratne. “Deformation of a peridynamic bar”. In: *Journal of Elasticity* 73.1 (2003), pp. 173–190.
- [3] Stewart A Silling, M Epton, O Weckner, Ji Xu, and E23481501120 Askari. “Peridynamic states and constitutive modeling”. In: *Journal of Elasticity* 88.2 (2007), pp. 151–184.
- [4] Ali Javili, Rico Morasata, Erkan Oterkus, and Selda Oterkus. “Peridynamics review”. In: *Mathematics and Mechanics of Solids* 24.11 (2019), pp. 3714–3739.
- [5] Florin Bobaru and Monchai Duangpanya. “The peridynamic formulation for transient heat conduction”. In: *International Journal of Heat and Mass Transfer* 53.19-20 (2010), pp. 4047–4059.
- [6] Xiaowei He, Huamin Wang, and Enhua Wu. “Projective peridynamics for modeling versatile elastoplastic materials”. In: *IEEE transactions on visualization and computer graphics* 24.9 (2017), pp. 2589–2599.
- [7] E. Madenci and E. Oterkus. *Peridynamic Theory and Its Applications*. SpringerLink : Bücher. Springer New York, 2013. ISBN: 9781461484653. URL: <https://books.google.co.in/books?id=r-63BAAQBAJ>.
- [8] J Sengupta, SL Cockcroft, D Maijer, MA Wells, and A Larouche. “The effect of water ejection and water incursion on the evolution of thermal field during the start-up phase of the direct chill casting process”. In: *Journal of Light Metals* 2.3 (2002), pp. 137–148.
- [9] Erkan Kreith F Black W Z. “Basic Heat transfer”. In: *Principles of Heat Transfer*. Cengage, 1980, pp. 19–43.
- [10] Stewart A Silling and Ebrahim Askari. “A meshfree method based on the peridynamic model of solid mechanics”. In: *Computers & structures* 83.17-18 (2005), pp. 1526–1535.
- [11] Erdogan Madenci and Erkan Oterkus. “Peridynamic theory”. In: *Peridynamic Theory and Its Applications*. 2014, pp. 19–43.
- [12] Duanfeng Han, Yiheng Zhang, Qing Wang, Wei Lu, and Bin Jia. “The review of the bond-based peridynamics modeling”. In: *Journal of Micromechanics and Molecular Physics* 4.01 (2019), p. 1830001.